Electrical evidence for the encapsulation of C_{60} inside a carbon nanotube: Random telegraph signal and hysteric current–voltage characteristics

Han Young Yu,[1,2] Dong Su Lee,[1,3] Ursula Dettlaff-Weglikowska,[3] Siegmar Roth,[3] and Yung Woo Park[1,*]
[1]*School of Physics, Seoul National University, Seoul 151-747, Republic of Korea and Nano Systems Institute–National Core Research Center, Seoul National University, Seoul 151-747, Republic of Korea*
[2]*Electronics and Telecommunications Research Institute, Daejeon 305-700, Republic of Korea*
[3]*Max-Planck-Institut für Festkörperforschung, Heisenbergstrasse 1, D-70569 Stuttgart, Germany*
(Received 20 May 2008; revised manuscript received 7 July 2008; published 10 October 2008)

We present electrical evidence for the encapsulation of C_{60}'s inside a carbon nanotube, random telegraph signals (RTSs), and hysteric current–voltage characteristics. RTSs are shown only at voltages higher than a critical voltage. We suggest that the origin of the RTSs is ascribed to the instability of the quantum harmonic oscillations of C_{60}'s. RTSs are smeared out at a temperature which is well correlated with the energy level of the vibrational quantum mediated by the van der Waals binding between the carbon nanotube and C_{60}'s. In addition, hysteric behavior in cyclic current–voltage characteristics is explained by the longitudinal motion and resettlement of the C_{60}'s with the modulation of the size of the quantum dot mediated by the C_{60} insertion.

DOI: 10.1103/PhysRevB.78.155415 PACS number(s): 73.63.−b, 62.25.−g, 73.23.Hk, 81.05.Tp

I. INTRODUCTION

Random current fluctuations as a function of time are often observed with existence of defect sites or of movable metallic particles in samples.[1–9] This current fluctuation, usually termed as random telegraph signal (RTS), is different from the typical $1/f$ noise: The current jumps from one value to another in some fixed current levels and the event is sudden and random. The RTSs have been reported in various devices: silicon metal-oxide semiconductor field-effect transistors,[1–4] carbon nanotubes with a single defect inside silicon dioxide or in the oxide-nanotube interface,[7] and metallic constrictions.[6] The origin of the RTS, however, is not yet clear although it is suggested to be the defects in the samples or in the oxide trapping and emitting charges.

The RTSs are also observed in electromechanical systems where movable islands act as charge shuttles between the source and drain electrodes.[8,9] In this case, the RTSs can serve as a direct indication of the island instability.[10–12] The instability is composed of two different regimes: *soft excitation* at low bias voltage and *hard excitation* at high bias voltage.[12] Here, we present electrical measurements on a C_{60} peapod showing RTSs. The RTSs are only observed at bias voltages larger than a critical voltage ($V > V_C$). We suggest that the vibration of C_{60}'s (soft excitation at low bias voltage) results in RTSs. Temperature-dependent RTS measurements also support the suggestion that the RTSs disappear at $T > 150$ K, where the thermal energy is the same as that of the quantum harmonic oscillations of C_{60}. Cyclic current–voltage (I-V) measurements up to much higher voltage show a hysteric behavior. In each cycle, the differential conductance peaks appear in different position, showing that the size of the quantum dot mediated by the C_{60} insertion is different from cycle to cycle. This can be explained by hard excitation, i.e., the longitudinal movement of C_{60}'s at high bias.

II. EXPERIMENT

C_{60} peapods[13,14] were synthesized as follows: Single wall carbon nanotubes (SWNTs) produced by laser ablation of carbon target containing 1 at. % Ni and 1 at. % Co as catalysts were prepared. The raw sample was purified by controlled thermal oxidation in air at 225 °C for 18 h, at 325 °C for 1.5 h, and 350 °C for 1 h followed by sonication in HCl to remove metallic impurities. The SWNTs were formed into thin bucky paper (6 mg), which was placed into a quartz ampoule. 35 mg of C_{60} was placed in a small quartz pot and put into the same ampoule. The ampoule was then evacuated to 10^{-6} torr and sealed. The pot with C_{60} was moved to the end of the ampoule opposite to the SWNTs bucky paper side. The ampoule was heated in a furnace with temperature gradient (600 °C at the fullerene side, 500 °C at the SWNT side) for 5 days. At this temperature C_{60}'s become mobile and condense on the SWNTs. The SWNT bucky paper was picked up, sonicated in toluene to dissolve fullerenes coated on the SWNT surface, filtrated, and dried. The peapods were dispersed in a 1 wt % sodium dodecyl sulfate (SDS)/water solution after sonication of the paper in the solution. In order to analyze the synthesized peapod, studies of high-resolution transmission electron microscopy (HRTEM) were conducted. From the HRTEM images we found that the C_{60}'s are not closely packed as those in the previously reported results[15] but more sparsely placed with an irregular spacing. The incomplete packing of C_{60}'s results in a multiple quantum dot structure.[16] Ti/Au (4 nm/10 nm) electrodes were patterned on a thermally grown SiO_2 (300 nm) substrate by electron-beam lithography. Highly n-doped Si was used as a back gate. After a small amount of the peapod solution was dropped on the chip, an ac voltage at 8 V peak to peak with 13 MHz was applied between the electrodes for 10 s to deposit the peapods.

A representative device is shown in the atomic force microscopy (AFM) image in Fig. 1(a). The length of the device is 400 nm (effective length of the C_{60} peapod) and the diameter is 2.3 nm. Figure 1(b) shows the schematic diagram of the C_{60} peapod device, where the C_{60} peapod is deposited on top of the metal electrodes.

 ©2008 The American Physical Society

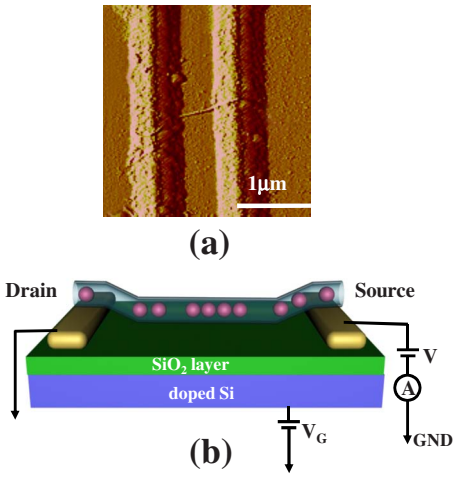

FIG. 1. (Color online) (a) A representative AFM image of a C_{60} device. (b) A schematic diagram of the C_{60} device circuit. A C_{60} peapod is deposited on top of the electrodes, a source electrode is connected to a voltage source and a current meter, and highly *n*-doped bottom silicon is connected to a gate.

III. RESULTS AND DISCUSSION

Current through the source and drain electrodes was monitored during application of various voltages at 1.8 K. Only above a critical voltage ($V_C \sim 0.9$ V) were RTSs with discrete current levels observed [Fig. 2(a)]. The switching frequency increases with increasing V_{DS}. The RTS behavior can also be seen in the $I-V$ curve [Fig. 2(b)]. The random current fluctuation is clear at high voltage. The current levels measured by the previous current monitoring are also plotted as a function of voltage in the figure for comparison (open diamonds). At $V_{DS} \geq V_C = 0.9$ V, two or more current levels are shown, whereas the current keeps a stable value at voltages below V_C.

In the previous report,[16] a C_{60} peapod worked as a quantum dot[17] after the electronic band modulations, featuring flattened electronic band in a pure carbon nanotube region as a *p*-type semiconductor and a modulated band in the C_{60} inserted region as quantum dots with variations of the Fermi level. Furthermore, C_{60}'s bound to a gold surface by van der Waals and electrostatic interaction oscillate at quantized energy levels.[18] Hence, C_{60} molecules inside a carbon nanotube also have vibrational quanta mediated by the van der Waals interaction with the inner surface of the carbon nanotube.[19,20] The corresponding binding energy between C_{60} and the carbon nanotubes for the samples (2–3 nm in diameter) ranges from 0.9 to 1 eV in Lennard-Jones potential.[20] Through this binding energy, quantum harmonic oscillation takes place near the minimum of the binding potential with a frequency of $f = \frac{\omega}{2\pi} = 3.07$ THz (vibrational quantum of $\hbar\omega = 12.7$ meV).[19] Thus, the electronic band of the C_{60} peapod is modified such that the subbands resulting from quantum harmonic oscillations are generated between the quantized energy levels of a quantum dot, between E_1 and E_2 as shown in Fig. 3.

As the bias voltage increases the Fermi level (E_F), as shown in Fig. 3, it aligns with the quantized energy level E_1

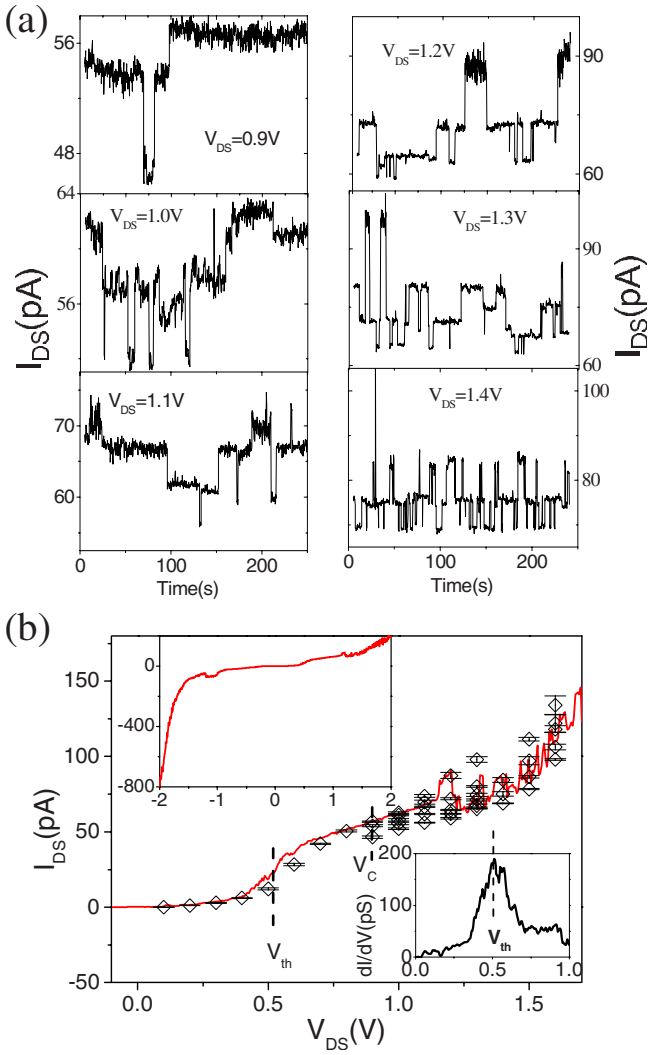

FIG. 2. (Color online) (a) Bias voltage dependence of the RTSs with applied voltages from 0.9 to 1.4 V at $T = 1.8$ K. (b) A plot of the averaged current levels deduced from the bias-voltage-dependent RTSs and an $I-V$ characteristic at $T = 1.8$ K: the threshold voltage V_{th} (0.51 V) and the critical voltage V_C, where the differential conductance shows peaks and discrete current levels appear, respectively. Upper inset: An $I-V$ characteristic with applied voltages ranging from −2 to 2 V at $T = 1.8$ K. Lower inset: Differential conductance curve. Comparing the behavior of $I-V$ characteristic (line) to the discrete current levels of the RTSs (diamonds), the fluctuations in the $I-V$ curve are well correlated with the deviations of the discrete RTS levels.

and the charges injected from the source reservoir tunnel into the state of E_1 and then tunnel out to the drain. While the bias voltage is further applied far from the V_{th} [Fig. 2(b)], the Fermi level aligns with the energy state of the vibrational quantum, and additional tunneling processes then occur (Fig. 3). The charges on the state of vibrational quantum, however, are unstable because the initial binding between the carbon nanotube and C_{60}'s is modified by the longitudinal electrostatic force. The applied electrostatic force gives rise to a significant change in the electronic structure of the C_{60} peapod due to the oscillations of the C_{60}'s. Sequential processes

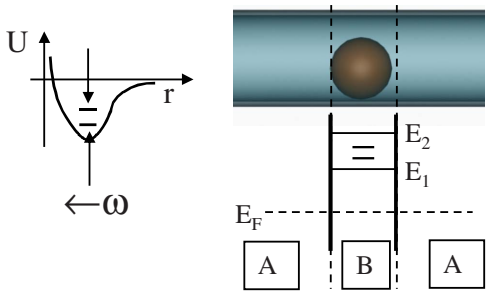

FIG. 3. (Color online) Left: Schematic diagram of the variation of the binding potential U with respect to the distance r from the inner wall of carbon nanotube to the surface of C_{60}. Right: Schematic diagram of the structure of a peapod with a single C_{60}, the electronic band diagram for the peapod quantum dot, and the resulting subband from the quantum harmonic oscillations (the energy of h) of C_{60} near the stable position in a direction perpendicular to the tube axis. A: Pure carbon nanotube region; B: C_{60} inserted region in a peapod; E_1 and E_2: The energy states mediated by the peapod quantum dot.

from stable to unstable oscillations of C_{60} appear when the bias voltage is higher than the electrostatic force between the C_{60} and the carbon nanotube. Through this instability of the C_{60} position and the modification of the electronic states, the measured current shows random fluctuations as a function of time, which can be compared to a scheme considered theoretically by Isacsson *et al.*[12] regarding shuttle instability in movable quantum dots.[10,11] They showed that electromechanical instability can develop as a consequence of the interplay between single electron tunneling and the mechanical vibration of metallic clusters with the longitudinal direction of the tunneling. When the applied voltage is higher than a certain critical voltage, soft and hard excitations of self-oscillation occur, in which the resulting current shows steps and hysteric behaviors in the $I-V$ curves due to the soft and the hard excitations, respectively.

The displacement of the C_{60} oscillations is limited to the soft excitation, whereas jump behavior occurs with the hard excitation depending on the pumping of the electrical energy into the system. Due to the ensemble between the soft excitation and van der Waals binding, the binding of C_{60} to the carbon nanotube is modified continually. As a result of this microscopic electromechanics, the current as a function of time appears as RTSs when the source-drain voltage is applied between the critical voltage of (V_C) and the hard excitation voltage of (V^*), $V^* > V_{DS} > V_C$, as shown in Fig. 2(a). However, at a low voltage bias of $V_{DS} < V_C$, the electrical results for the C_{60} peapod did not show random current fluctuations.[15,16,21] No fluctuations were observed because the electronic structure modified by the C_{60} insertion is not close to the Fermi level.[22] The electrical effects including the oscillation of the C_{60} occur only at a high voltage bias as a form of RTS.

In order to verify the RTS variations in terms of temperature dependency, RTSs were measured at temperatures ranging from $T=1.8$ to 300 K with fixed source-drain voltage of 1.3 V as shown in Fig. 4. As the temperature increased, the switching frequency between discrete RTS levels increased

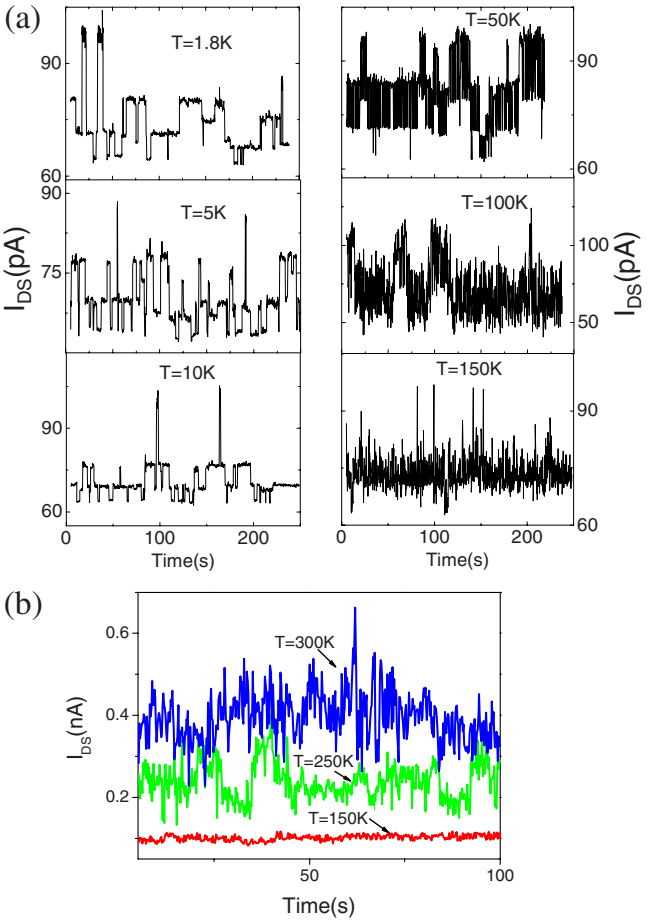

FIG. 4. (Color online) (a) Temperature-dependent RTSs with a source-drain voltage of 1.3 V. (a) Discrete current levels appear at temperatures ranging from 1.8 to 100 K. (b) Current fluctuations without quantized levels at temperatures from 200 to 300 K.

below a critical temperature of $T \simeq 150$ K. The RTS signals become spread out at $T > 150$ K. This behavior is related to the thermal broadening of the vibrational quantum, $\hbar\omega = 12.7$ meV. Thus in order to understand the correlations between the RTS and the temperature, the RTS results should be considered in the two different temperature regimes of $k_BT < \hbar\omega$ and $k_BT \geq \hbar\omega$.

In the *low-temperature regime* $(k_BT < \hbar\omega)$, because the thermal energy is lower than the energy of the quantum harmonic oscillation, conduction occurs mainly through the quantized states mediated both by the quantum dot and the quantum harmonic oscillations. As the discrete level spacing of the quantum dot, $\Delta E_n = E_n - E_{n-1}$, is larger than the thermal energy at the Coulomb blockade regime, $\Delta E_n \gg k_BT$, the lowest current levels are independent of the temperature at the low-temperature regime, as shown in Fig. 5. In addition, because the applied voltage $(V_{DS} = 1.3$ V) is higher than the critical voltage $(V_C \simeq 0.9$ V), RTSs are clearly shown in the temperature range of $T = 1.8$ K to $T = 150$ K [Fig. 4(a)].

On the other hand, in the *high-temperature regime* $(k_BT \geq \hbar\omega)$, the subbands of the vibrational quanta are broadened and merge into the nearest state of the quantum dot. As a result of the broadening of the electronic band, RTSs are not

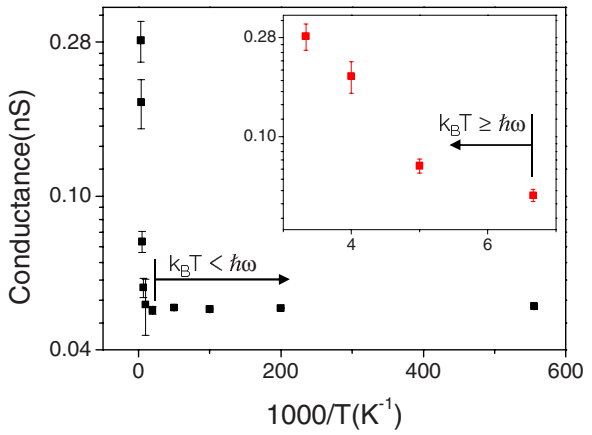

FIG. 5. (Color online) Plot of the conductance in the discrete RTS levels as a function of temperature from 1.8 to 300 K at $V_{SD}=1.3$ V. Inset shows RTS levels above critical temperature of 150 K.

observed in this regime and the conductance as a function of the temperature increases exponentially as shown in the inset of Fig. 5.

For further investigation of the movements of C_{60}'s in a high electric field of $V_{DS} \geq V^*$, experiments on the current responses at high bias voltages of up to 3.7 V were done at $T=1.8$ K. The applied voltage ranged from 0 to 3.7 V and moved back down to 0 V repeatedly, as shown in Fig. 6(a). At the first step (up1), the induced current increases monotonously and two conductance peaks appear in the differential conductance curve [inset of Fig. 6(b)] below $V_{DS}=2$ V. The current, however, increases abruptly above $V_{DS} \sim 3.5$ V. Sweeping the voltage down from $V_{DS}=3.7$ V to 0 V (down1), two level fluctuations appear above $V_{DS} \sim 3.0$ V and the current decreases monotonously, and two staircases are shown below $V_{DS} \sim 1.0$ V. During the up2 step, the current behavior is similar to that of down1 and shows abnormal behavior at a high voltage bias, $V_{DS} \sim 3.6$ V. In addition, feature of the current in the down2 step differs from that of the up2 step.

These behaviors in a high electric field are well correlated with the current behavior under hard excitation.[12] When the applied voltage is exceedingly high compared to the critical voltage and hard excitation voltage ($V_{DS} \geq V^* \gg V_C$), the displacement of the oscillating beads increases abruptly and the resulting current shows a discrete jump with increase in the voltage. Additionally, it re-enters another current level while the voltage is lowered.

From the differential conductance curves [Fig. 6(b)], it is clear that the energy level spacing $2\Delta E$ changes as the voltage-sweep sequences continue. At up1 step, $2\Delta E_1 = 0.377$ eV; at the up2 (down1) step, $2E_2=0.537$ eV; and at the down2 step, $2\Delta E_3=1.274$ eV. The energy level spacing related to the size of a quantum dot increases with the cycling measurements, indicating that the size of the quantum dot is miniaturized inversely. These results also support that the quantum dot and RTSs do not originate from the contact resistance or the defects around the peapod but from the electronic modulation of the peapod by the C_{60} insertion, as the size of the quantum dot in a contact-oriented carbon

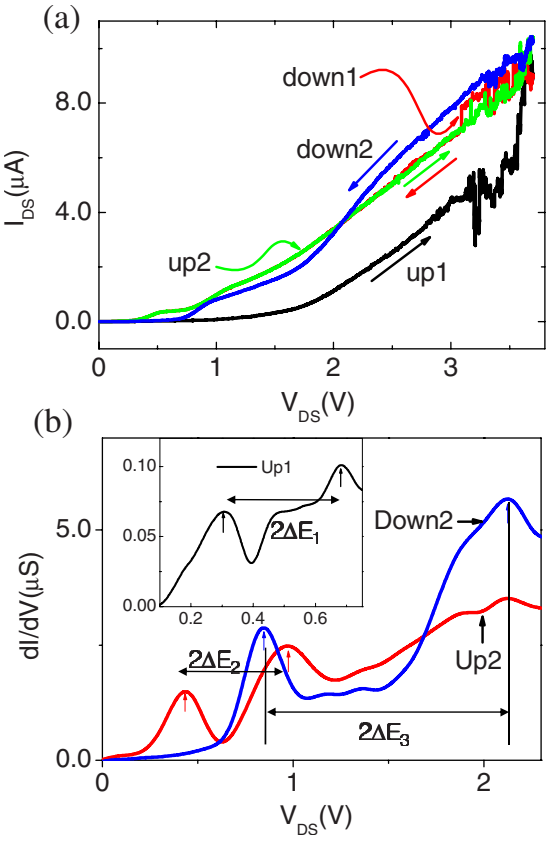

FIG. 6. (Color online) (a) Cyclic $I-V$ characteristics of a C_{60} peapod device at $T=1.8$ K. The induced current was measured under the following sequence of voltage sweeps: up1, down1, up2, and down2. (b) Differential conductance curves to the applied source-drain voltage. Arrows indicate conductance peaks at each differential conductance.

nanotube single electron transistor could not be changed, even in a high electric field.

IV. CONCLUSION

This study presents electrical evidence that confirms quantum oscillations and the hysteric displacement of C_{60}'s inside a carbon nanotube. The findings are as follows: (i) When the applied electrostatic potential is under the binding potential between C_{60} and the carbon nanotube, the current as a function of time shows RTSs, indicating that the quantum harmonic oscillations of the C_{60} mediate the random fluctuation of current (soft excitation). (ii) The energy of the temperature at which the RTSs were spread out was identical to that of the vibrational quantum. This suggests that the RTSs originate from the quantum harmonic oscillation of C_{60}. (iii) From the hysteric $I-V$ curves up to a high voltage bias, it was shown that the position of the C_{60}'s is modified by the perturbation of the external electric field (hard excitation).

In general, when the nanoscaled devices composed of movable clusters are linked to the source-drain electrodes and/or when the nanobeads are encapsulated by a nanotube, the empirical results of the RTSs and hysteric $I-V$ character-

istics will appear in electrical measurements, which can also be adopted to support a spectroscopic analysis. Moreover, these results suggest that the use of peapodlike systems as nonvolatile memory devices is feasible. From the hysteric behavior in the $I-V$ curve, the off and on states in the up and down sweeps, respectively, can be defined.

ACKNOWLEDGMENTS

This work was supported by the Korea Foundation for International Cooperation of Science and Technology (KICOS) through a grant provided by the Ministry of Education, Science and Technology (MEST), Korea (Grant No. GPP K20602000006-07E0200-00610).

*Author to whom correspondence should be addressed.
ywpark@phya.snu.ac.kr

[1] M. A. Kastner, R. F. Kwasnick, J. C. Licini, and D. J. Bishop, Phys. Rev. B **36**, 8015 (1987).
[2] M. J. Uren, M. J. Kirton, and S. Collins, Phys. Rev. B **37**, 8346 (1988).
[3] Sh. Kogan, *Electronic Noise and Fluctuations in Solids* (Cambridge University Press, Cambridge, United Kingdom, 1996).
[4] B. L. Altshuler, P. A. Lee, and R. A. Webb, *Mesoscopic Phenomena in Solids* (Elsevier Science, New York/North-Holland, Amsterdam, 1991).
[5] M.-E. Pistol, P. Castrillo, D. Hessman, J. A. Prieto, and L. Samuelson, Phys. Rev. B **59**, 10725 (1999).
[6] K. S. Ralls and R. A. Buhrman, Phys. Rev. Lett. **60**, 2434 (1988).
[7] F. Liu, M. Bao, H.-j. Kim, K. L. Wang, C. Li, X. Liu, and C. Zhou, Appl. Phys. Lett. **86**, 163102 (2005).
[8] N. Nishiguchi, Phys. Rev. Lett. **89**, 066802 (2002).
[9] N. Nishiguchi, Jpn. J. Appl. Phys., Part 1 **40**, 1923 (2001).
[10] L. Y. Gorelik, A. Isacsson, M. V. Voinova, B. Kasemo, R. I. Shekhter, and M. Jonson, Phys. Rev. Lett. **80**, 4526 (1998).
[11] T. Nord, L. Y. Gorelik, R. I. Shekhter, and M. Jonson, Phys. Rev. B **65**, 165312 (2002).
[12] A. Isacsson, L. Y. Gorelik, M. V. Voinova, B. Kasemo, R. I. Shekhter, and M. Jonson, Physica B (Amsterdam) **255**, 150 (1998).
[13] B. W. Smith and D. E. Luzzi, Chem. Phys. Lett. **321**, 169 (2000).
[14] G.-H. Jeong, R. Hatakeyama, T. Hirata, K. Tohji, K. Motomiya, N. Sato, and Y. Kawazoe, Appl. Phys. Lett. **79**, 4213 (2001).
[15] C. H. L. Quay, J. Cumings, S. J. Gamble, A. Yazdani, H. Kataura, and D. Goldhaber-Gordon, Phys. Rev. B **76**, 073404 (2007).
[16] H. Y. Yu, D. S. Lee, S. H. Lee, S. S. Kim, S. W. Lee, Y. W. Park, U. Dettlaff-Weglikowskaand, and S. Roth, Appl. Phys. Lett. **87**, 163118 (2005).
[17] H. Grabert and M. H. Devoret, *Single Charge Tunneling* (Plenum, New York, 1992).
[18] H. Park, J. Park, A. K. L. Lim, E. H. Anderson, A. P. Alivisatos, and P. L. McEuen, Nature (London) **407**, 57 (2000).
[19] R. S. Ruoff and A. P. Hickman, J. Phys. Chem. **97**, 2494 (1993).
[20] L. A. Girifalco, M. Hodak, and R. S. Lee, Phys. Rev. B **62**, 13104 (2000).
[21] P. Utko, J. Nygård, M. Monthioux, and L. Noé, Appl. Phys. Lett. **89**, 233118 (2006).
[22] D. J. Hornbaker, S.-J. Kahng, S. Misra, B. W. Smith, A. T. Johnson, E. J. Mele, D. E. Luzzi, and A. Yazdani, Science **295**, 828 (2002).